LA-UR-20-27416
Approved for public release; distribution is unlimited.

Title: CALCULATION OF THE FIRST MOMENT OF ENERGY USING D-T REACTIVITY FORMALISMS UNDER THE MAXWELL-BOLTZMANN DISTRIBUTION—PART I

Author(s): Langenbrunner, James R.
Booker, Jane M.

Intended for: Report

Issued: 2020-09-22

CALCULATION OF THE FIRST MOMENT OF ENERGY USING D-T REACTIVITY FORMALISMS UNDER THE MAXWELL-BOLTZMANN DISTRIBUTION—PART I

August 20, 2020
James R. Langenbrunner & Jane M. Booker
Los Alamos National Laboratory and Booker Scientific

Abstract

Nuclear fusion science is an example of a scientific field with a rich history of expert involvement and scientific publications, which together, form an expert-knowledge base. One example of this history is the utilization of published reaction rates from a variety of authors. Investigators for Deuterium-Tritium (D-T) ion fusion can choose from using frequently cited methods: the Bosch and Hale [1] reactivity, thermonuclear reaction rates from Caughlan and Fowler [2], and the reactivity evaluation from Miley, Towner & Ivich [3] which forms the basis of the Naval Research Lab (NRL) formulary [4]. There are other choices available. Each of the reactivity formulations considered here, [1-4], are based upon the Maxwell-Boltzmann velocity distribution for D-T fusion ion reactants. Numerical methods for computer codes simulating hot, energetic plasmas, include tabulations of the reactivity, and the first moment of energy. The purpose of this study is to answer the question: what is the first moment of energy, and how has it been formulated?

This report is part of a series of reports by the authors on D-T fusion-reaction formalism, [5-9]. The present focus is on defining the mathematical relationship of the first moment of D-T fusion ion kinetic energy, $\langle E \rangle$, with the fusion cross-section, fusion reactivity and its derivative with respect to ion-temperature. Three variants of the first moment $\langle E \rangle$ are analytically developed and explored: 1) constant cross-section, 2) a normalized first moment, and 3) a particular function of the first moment. Much of the mathematical development is relegated to the Appendices, for a concise presentation of topics and results. A research component of this discussion is our comparison of some of the reactivity and its derivative results between evaluations [1] versus [2] and [3], which the authors have not found in any other publication to date. This investigation is useful for validation, verification (V&V) and uncertainty quantification (UQ) as it compares the work of several authors.

I. Introduction—Reactivity & Energy

There exist a multitude of useful, published evaluations of Deuterium-Tritium (D-T) ion fusion reaction rates, for example, References [1-4]. Reasoning for preferring one evaluation to another is not usually explained by authors/experts. The reasons which could cause a scientist to prefer one evaluation over another include validity, confidence, or ease of use. Nuclear fusion is a scientific field with a rich history of expert involvement and *scientific* publications, which together, form an expert-knowledge base. As can happen,

jargon and historical standards can reduce the transparency of a subject, making validation, verification and uncertainty quantification difficult. The focus of this paper is on defining the *mathematical* relationship of the first moment of D-T fusion-ion kinetic energy, <*E*>, with the cross-section for D-T fusion. This technical note is one in a series of reports ([5], [6], [7], [8], [9]) examining various aspects of reactivity formalisms of fusion physics and mathematical methods, interrelationships of physical quantities and observables, analyses results, and references. The D-T fusion reaction is especially interesting because it lends itself to practical use. In the jargon of nuclear physics, it is a large, broad, charged-particle resonance reaction. Under the physical applications assumed for this discussion, all nuclei and radiation are in thermodynamic equilibrium under nondegenerate, nonrelativistic conditions with regards to velocity and energy distribution.

Fusion reactivity, f, is traditionally expressed as the average over the Maxwell-Boltzmann (MB) velocity distribution for ions, $g(v)$,

$$f = <\sigma v> = \int_0^\infty \sigma(v) v g(v)\, dv = \int_0^\infty \sigma(v) v 4\pi \left(\frac{m}{2\pi k T^\circ}\right)^{1.5} v^2 \exp\left(\frac{-mv^2}{2kT^\circ}\right) dv \quad (1)$$

where the MB velocity probability density function (pdf) is:

$$g(v)dv = 4\pi \left(\frac{m}{2\pi k T^\circ}\right)^{1.5} v^2 \exp\left(\frac{-mv^2}{2kT^\circ}\right) dv \quad . \quad (2)$$

This is the same assumption made for the ideal gas, comprised of atoms or molecules. The MB pdf in (2) can be considered as the probability per unit speed, v, and is the chi distribution (positive square root of the chi-squared pdf) with 3 degrees of freedom [10].

The velocity, v, is the magnitude of speeds in three directions, x, y and z, and is defined as:

$$v = \sqrt{{v_x}^2 + {v_y}^2 + {v_z}^2}\,. \quad (3)$$

Each speed in (3) can be defined as a relative velocity, the absolute value of the difference of two speeds. The development of the MB pdf in (2) is given in Appendix A starting from the distribution for a single species of speed. The single direction of speed distribution is commonly known as the Boltzmann distribution or the Maxwell distribution [10].

In (1) and (2), T° is in units of °K, degrees Kelvin, and $\sigma(v)$ is the cross-section as a function of velocity. Ion-temperature, T, is expressed in keV, and corresponds to the product kT° in (1) and (2). The value of the Boltzmann constant is k = 8.612 x 10^{-8} keV/°K. From this point on, kT° is expressed as T. Reactivity, expressed in (1), has dimensions of volume/time, and for the scaling used here, those units are cm^3/sec. The mass, m, is the reduced mass, which for two masses, m_1 and m_2 is given by:

$$m = \frac{m1m2}{m1+m2} \quad . \quad (4)$$

The development of reactivity, *f*, in (1) is also given in Appendix A. It begins with two traditional definitions of velocity: center-of-mass (CM) and relative velocity. Of those two, only the relative velocity is preserved in (1).

There is another frequently cited formulation for reactivity in (1) based upon energy instead of velocity. References include Bosch and Hale [1], Kaye & Laby [11], Brysk [12], Fowler et al. [13] and Miley et al. [3]. This *E* formulation relies upon the relative kinetic energy

$$E = \left(\frac{1}{2}\right) m v^2 \tag{5}$$

where *m* is reduced mass in (4) and *v* is in (3). This kinetic energy definition with this mass definition is the center of mass energy, or E_{CM}. The energy formulation is often used in conjunction with the astrophysical factor, $S(E)$ [1, 2] discussed in following sections.

This energy formulation in (5) can also be mathematically expressed using momentum, *p*,

$$E = \left(\frac{|p|^2}{2m}\right). \tag{6}$$

The relationship between energy and velocity in (5) is used to find the distribution for *E* from the MB pdf in (2) applying the change of variable technique (from *v* to *E*). That development is in Appendix B.

The MB energy distribution is:

$$g(E) = 2\left(\frac{E}{\pi}\right)^{1/2}\left(\frac{1}{T}\right)^{3/2} exp\left(-\frac{E}{T}\right). \tag{7}$$

Wikipedia® [10] provides the development of (7) from the momentum in (4).

The energy distribution in (7) looks similar to the two-parameter (κ, θ) gamma pdf for random variable *x* given in (8):

$$\mathrm{gamma}(\kappa, \theta) = \frac{x^{(\kappa-1)}}{\Gamma(\kappa)\theta^{\kappa}} exp\left(-\frac{x}{\theta}\right). \tag{8}$$

Comparing (7) to (8) reveals $g(E)$ is a gamma pdf, where the random variable, *x*, is *E,* and *T* is the scale parameter θ. The shape parameter of κ is 3/2. The leading square root term of (7) matches that of the gamma pdf because $\Gamma(3/2)=1/2\sqrt{\pi}$.

The mean of $g(E)$, when $g(v)$ is the MB distribution, is $\kappa\theta = 3T/2$. This latter result is familiar from elementary physics texts: The average translational kinetic energy of an object mass *m* is 3/2 $kT°$ [here defined as ion-temperature, *T* (keV)]. The variance, is $\kappa\theta^2 = 3T^2/2$.

While $g(E)$ being a gamma pdf when $g(v)$ is the MB pdf is an interesting result, the major focus of this series of technical report is on reactivity, $f = \langle \sigma v \rangle$, in (1), and its derivatives with T.

Obtaining the reactivity (1) in terms of E follows from the change of variable (v to E) with the velocity pdf (2) conversion to the energy pdf (5). Beginning with reactivity in (1), the substitution for v in terms of E comes from (5) and for $g(v)$ comes from $g(E)$ in (7). The latter comes from the change of variable technique in Appendix B which accounts for the change of dv to dE through the Jacobian. The resulting reactivity in terms of E becomes:

$$f = \int_0^\infty \sigma(v) \cdot v \cdot g(v)\, dv = \int_0^\infty \sigma(E) \sqrt{\frac{2E}{m}} \cdot g(E)\, dE$$

$$f = \int_0^\infty \sigma(E) \sqrt{\frac{2E}{m}} \cdot 2 \left(\frac{E}{\pi}\right)^{1/2} \left(\frac{1}{T}\right)^{3/2} exp\left(-\frac{E}{T}\right) dE$$

$$f = \left(\frac{1}{T}\right)^{3/2} \int_0^\infty \sigma(E) \cdot E \sqrt{\frac{8}{m\pi}} \cdot exp\left(-\frac{E}{T}\right) dE \qquad (9)$$

Moving the square root term outside the integral (9) produces the familiar form for the reactivity in terms of E as:

$$f = \left(\frac{8}{\pi m}\right)^{1/2} \left(\frac{1}{T}\right)^{3/2} \int_0^\infty \sigma(E) E \exp\left(\frac{-E}{T}\right) dE\,. \qquad (10)$$

This reactivity expression can be found in the literature, especially in the astrophysics community. For example, see page 86 of Fowler *et al*. [13].

A side by side comparison of (10) and (1) shows the similarity of the two reactivity forms:

$$\left(\frac{2}{\pi}\right)^{1/2} \left(\frac{m}{T}\right)^{3/2} \int_0^\infty \sigma(v)\, v^3 \exp\left(\frac{-mv^2}{2T}\right) dv = \left(\frac{8}{\pi m}\right)^{1/2} \left(\frac{1}{T}\right)^{3/2} \int_0^\infty \sigma(E) E \exp\left(\frac{-E}{T}\right) dE. \qquad (11)$$

With various calculation formulations for f in terms of velocity available (*e.g.,* [1], [2], [4]), examining the relationship between these two forms is interesting. Much of the experimental, observational and computational focus of reactivity uses the energy formulation. The derivatives of f with T, *e.g.* [5-8], drives the need to understand the comparison between the two reactivity forms in (11).

II. First Moment Definition for *E*

The expected value or mean (or average) for a continuous random variable x distributed as the probability density function, $g(x)$, is given as:

$$< x_{avg} > = \int_{-\infty}^{\infty} x g(x)\, dx. \tag{12}$$

The probability distribution, $g(x)$, has the requirement that its integral equals 1:

$$\int_{-\infty}^{\infty} g(x)\, dx = 1 \ . \tag{13}$$

Equation (12) is the average of x, and the integration is over all admissible values of x. This expected value of x is also known as the mean of x, the average value of x, and the first moment of the distribution function, $g(x)$.

Many physical variables, like energy and reactivity, do not have negative values making the lower integral limit 0 in (12)-(13).

As used in physical applications, the intention of (13) is that the summation of probabilities of observing each possible final state (outcomes) over all "trials" is defined as 1.

The probability of observing the random variable between limits x_1 and x_2 is:

$$P(x_1 \leq \ x \leq x_2) = \int_{x1}^{x2} g(x)\, dx \ . \tag{14}$$

The integrands and the integrals cannot be greater than one or less than zero in (13) and (14).

If the constraint in (13) is lifted, then a general first moment for x can be defined using any general function of x, $h(x)$. The general first moment of x is defined using the same notation as:

$$< x >= \int_{-\infty}^{\infty} x h(x)\, dx \ , \tag{15}$$

where there are no restrictions on $h(x)$.

Only when $g(x)$=$h(x)$ is the first moment also the mean or average in (12). In this case, the units of $<x_{avg}>$ match those of x. In the general case in (15), this is not necessarily the case.

As an example, it is usual for beginning physics students to make the analogy with mass moments. In this case, the mean, or first moment, represents the center-of-mass of the mass distribution [$g(x)$ is the mass distribution function in this example]. The random variable x corresponds to the position in one dimension, the distance to the origin, defined in the chosen coordinate system. [In this example, position x could take on negative values, but

mass cannot take on negative values.] Evaluation of the integral in (12) yields the center-of-mass in this example.

The reactivity, $<\sigma v>$, in (1) uses the general first moment notation where x is a compound quantity, $\sigma(v)\cdot v$, and $h(x)$ is the MB velocity distribution function in (2). Notice that while the MB distribution is a pdf, it is not the distribution function of the compound variable $\sigma(v)\cdot v$—MB is the distribution function only of velocity. Technically, reactivity is not an expected value or mean as in (12) unless the MB pdf is considered as the joint distribution of $\sigma(v)\cdot v$. The form of the reactivity integral in (1) is velocity oriented:

$$f =< \sigma v >= \int_0^\infty \{\sigma(v) \cdot v\} g(v)\, dv.$$

Nonetheless, reactivity in (1) can be considered as a measure of central tendency of the compound quantity, and $<\sigma(v)\cdot v>$ has units of $\sigma(v)\cdot v$.

Reactivity defined in terms of E in (10) has the form of the general first moment in (15) with the presence of $\sigma(E)$. Everything in the integrand is in terms of E:

$$f = \left(\frac{8}{\pi m}\right)^{1/2} \left(\frac{1}{T}\right)^{3/2} \int_0^\infty \sigma(E) E \exp\left(\frac{-E}{T}\right) dE.$$

Reactivity, written above in terms of E, produces an equation for the general first moment of energy, $<E>$, as:

$$\int_0^\infty \sigma(E) E \exp\left(\frac{-E}{T}\right) dE = \int_0^\infty E\, h(E)\, dE =< E >. \tag{16}$$

In (16), $h(E)$ is assigned as:

$$h(E) = \sigma(E)\exp\left(\frac{-E}{T}\right) \ . \tag{17}$$

Then reactivity (10) can be expressed in terms of $<E>$ in (16) using (17) as:

$$f = \left(\frac{8}{\pi m}\right)^{1/2} \left(\frac{1}{T}\right)^{3/2} \int_0^\infty \sigma(E) E \exp\left(\frac{-E}{T}\right) dE = \left(\frac{8}{\pi m}\right)^{1/2} \left(\frac{1}{T}\right)^{3/2} \int_0^\infty h(E)\, dE$$

$$f = \left(\frac{8}{\pi m}\right)^{1/2} \left(\frac{1}{T}\right)^{3/2} < E >. \tag{18}$$

For convenience, inclusion of the constant term in reactivity, C,

$$C = \left(\frac{8}{\pi m}\right)^{1/2},$$

will be suspended:

$$f = C \left(\frac{1}{T}\right)^{3/2} < E >= \left(\frac{1}{T}\right)^{3/2} < E > \ . \tag{19}$$

Analytically[1] evaluating the integral in (16) is difficult because the cross-section can, in general, be a complicated function of the energy. Assuming a constant cross-section mitigates the mathematical difficulty. This special case is examined below, as an example. The case for preserving $\sigma(E)$ inside the integral is that the probability for the D-T fusion reaction varies significantly with energy over the widths of the distributions. This effect is particular for D-T fusion as a function of temperature, given the low-lying resonance. That development is continued in a subsequent paper by the authors, labeled as Part II. It should be noted that few forms of the cross-section can be analytically integrated.

III. Reactivity Temperature Derivative

The focus of this study continues that of previous studies [5, 7] which is on the ion-temperature derivative of reactivity. This quantity will prove useful for diagnostics:

$$f'=df/dT, \tag{20}$$

The reactivity T derivative using $<E>$ in (20) is

$$f' = \frac{df}{dT} = \frac{d(T^{-3/2}\int_0^\infty E\sigma(E)\exp(-E/T)\cdot dE))}{dT} = \frac{d\left(T^{-3/2}<E>\right)}{dT}$$

$$f' = -\frac{3}{2}\left(\frac{1}{T}\right)^{\frac{5}{2}} < E > + \left(\frac{1}{T}\right)^{3/2}\frac{d(<E>)}{dT} \quad . \tag{21}$$

A previous study in this series, [5], explored the reactivity T derivative, and the ratio of f'/f in particular. That ratio for $<E>$ becomes:

$$\frac{f'}{f} = \frac{-\frac{3}{2}\left(\frac{1}{T}\right)^{\frac{5}{2}}<E>+\left(\frac{1}{T}\right)^{3/2}\frac{d(<E>)}{dT}}{\left(\frac{1}{T}\right)^{3/2}<E>} = -\frac{3}{2}\left(\frac{1}{T}\right) + \left(\frac{1}{<E>}\right)\frac{d(<E>)}{dT} \quad . \tag{22}$$

Noting that

$$\frac{1}{<E>} = \frac{d[\ln(<E>)]}{d(<E>)}, \tag{23}$$

substitute (23) for $1/<E>$ in (22) to produce an f'/f ratio expression that can be calculated from the ion-temperature T, reactivity, and its first T derivative, f':

$$\frac{f'}{f} = -\frac{3}{2}\left(\frac{1}{T}\right) + \frac{d(<E>)}{dT}\frac{d[\ln<E>]}{d<E>} = -\frac{3}{2T} + \frac{d[\ln(T^{1.5}f)]}{dT} \quad . \tag{24}$$

[1] Numerical methods of evaluation are not considered here. Hale & Talley [14] use the computer code STEEPM for numerical integration.

The last term in (24) is a result of $< E >= T^{1.5} f$, from (18), without the leading constant, *C*. Therefore, the f'/f ratio is a function of the first moment, <*E*>.

As noted earlier, three special cases of the first moment of <*E*> are examined:

1. Assume a constant cross-section, σ, which does not vary with *E*.
2. Normalize the general function, *h*(*x*), in (19) to produce the average as in (12).
3. Examine the f'/f ratio expression in (24) in conjunction with the solution and definition of <*K*> from Brysk [12].

Case 1: Constant Cross-section

For a constant σ, not a function of *E*, there is no cross-section inside the integral, and *h*(*E*) is defined as:

$$h(E) = \frac{1}{T}\exp(-E/T). \tag{25}$$

If a (1/*T*) term is pulled inside the integral, as in (25), the first moment of energy becomes analytically tractable. The first moment of energy for this case is designated as <E^*>:

$$< E^* >= \int_0^\infty \frac{1}{T} E\exp(-E/T)\, dE. \tag{26}$$

The reactivity designated as f^* becomes:

$$f^* = \left(\frac{8}{\pi m}\right)^{1/2} \left(\frac{1}{T}\right)^{1/2} \sigma \int_0^\infty \frac{1}{T} E\exp(-E/T)\, dE. \tag{27}$$

The relationship between the first moment (26) and reactivity (28) for the constant cross-section case is:

$$f^* = \left(\frac{8}{\pi m}\right)^{1/2} \left(\frac{1}{T}\right)^{\frac{1}{2}} \sigma < E^* >= C \left(\frac{1}{T}\right)^{\frac{1}{2}} \sigma < E^* >= \left(\frac{1}{T}\right)^{\frac{1}{2}} \sigma < E^* >. \tag{28}$$

Again, the leading constant *C* is temporarily dropped.

The reactivity integral in (27) has a closed form. That integral is the mean of the exponential pdf. This result is also useful for determining the $\frac{d(<E>)}{dT}$ when evaluating the reactivity *T* derivative in (21).

Restoring the leading *C* and constant cross-section, the reactivity derivative with respect to *T* is as follows:

$$f^{*\prime} = C\sigma \frac{d\left(\left(\frac{1}{T}\right)^{1/2} < E^* >\right)}{dT} = C\sigma \left(\frac{1}{T}\right)^{1/2} \frac{d < E^* >}{dT} + < E^* > \frac{d\left(\left(\frac{1}{T}\right)^{1/2}\right)}{dT}. \quad (29)$$

The derivative in the second term is evaluated as:

$$\frac{d\left(\left(\frac{1}{T}\right)^{1/2}\right)}{dT} = \frac{d(T^{-1/2})}{dT} = -0.5T^{-3/2}. \quad (30)$$

The derivative in the first term is evaluated using $<E^*>=T$:

$$\frac{d < E^* >}{dT} = \frac{dT}{dT} = 1. \quad (31)$$

Then $f^{*\prime}$becomes

$$\frac{f^{*\prime}}{C\sigma} = T^{-1/2} - 0.5 < E^* > T^{-\frac{3}{2}}, \quad (32)$$

or alternatively as:

$$\frac{f^{*\prime}}{C\sigma} = T^{-5/2}T^2 - 0.5 < E^* > T^{-\frac{3}{2}} = T^{-5/2} < E^* >^2 - 0.5 < E^* > T^{-\frac{3}{2}} \quad . \quad (33)$$

The final form of $f^{*\prime}$ from (33) is:

$$f^{*\prime} = C\sigma\left(-0.5T^{-3/2} < E^* > + T^{-5/2} < E^* >^2\right) \quad .$$

Recall that:

$$f^* = C\sigma T^{-1/2} < E^* >;$$

therefore, the ratio is

$$\frac{f^{*\prime}}{f^*} = \frac{\left(-\frac{1}{2}\left(\frac{1}{T}\right)^{3/2} < E^* > + \left(\frac{1}{T}\right)^{5/2} < E^* >^2\right)}{\left(\frac{1}{T}\right)^{\frac{1}{2}} < E^* >} = \frac{-1}{2T} + \frac{< E^* >}{T^2} \quad (34)$$

with $C{\cdot}\sigma$ cancelling out in numerator and denominator.

There is an equivalent analytical formulation in Appendix C featuring an alternative form of $h(E)$ as:

$$h(E) = \exp(-E/T). \quad (35)$$

Case 2: Normalization to Produce the First Moment as the Mean

The first moment in its general form is defined in (15) as:

$$< x >= \int_{-\infty}^{\infty} x h(x)\, dx \ .$$

The general first moment of energy, <*E*>, is in (16) as:

$$\int_0^{\infty} \sigma(E) E \exp\left(\frac{-E}{T}\right) dE = \int_0^{\infty} E\ h(E)\, dE =< E > \ .$$

Examination of (16) indicates that the units of <*E*> are cm^2 keV^2 where *E* has units of keV and cross-section has units of cm^2. One would rather have the first moment with units matching those of the *E*, which are keV. When the moment corresponds to the expected value, mean or average of *E*, then the units match. Recall, the expected value for a continuous random variable *E* distributed as the probability density function (pdf), $g(E)$, is given as in (12) as:

$$< E_{avg} >= \int_0^{\infty} E g(E)\, dE, \tag{35}$$

where, $g(E)$, is a pdf with the requirement that it integrates to 1,

$$\int_0^{\infty} g(E)\, dE = 1 \ .$$

To convert the general function $h(E)$ to a pdf, $g(E)$, requires normalization: change

$$\frac{h(E)dE}{\int_0^{\infty} E\ h(E)dE} = g(E). \tag{36}$$

The units of $g(E)$ are inverse those of *E*, keV, and the mean or average of *E* is designated as <E_{avg}>:

$$< E_{avg} >= \int_0^{\infty} E\ [\sigma(E) \exp\left(\frac{-E}{T}\right) / \int_0^{\infty} \sigma(E) \exp\left(\frac{-E}{T}\right) dE]\, dE \tag{37}$$

The normalizing integral in the denominator is a constant with respect to *E* but is a function of *T*. It is designated as $1/A(T)$:

$$\frac{1}{A(T)} = \int_0^{\infty} \sigma(E) \exp\left(\frac{-E}{T}\right) dE$$

$$< E_{avg} >= A(T) \int_0^{\infty} E\sigma(E) \exp\left(\frac{-E}{T}\right) dE$$

$$< E_{avg} >= A(T) < E > \quad . \tag{38}$$

The units of <E_{avg}> are now the same as *E*, keV, as demonstrated by the ratio in (37).

Reactivity for the general first moment is given in (10) as:

$$f = \left(\frac{8}{\pi m}\right)^{1/2}\left(\frac{1}{T}\right)^{3/2} < E >.$$

Reactivity for $<E_{avg}>$ is now

$$f = \left(\frac{8}{\pi m}\right)^{1/2}\left(\frac{1}{T}\right)^{3/2}\frac{A(T)}{A(T)}\int_0^\infty E\sigma(E)\exp\left(\frac{-E}{T}\right)dE$$

$$f = \frac{C}{A(T)}\left(\frac{1}{T}\right)^{3/2} < E_{avg} > \ , \tag{39}$$

where C is the same leading constant as before, $\left(\frac{8}{\pi m}\right)^{1/2}$.

The $<E_{avg}>$ is a desirable definition for the first moment because it corresponds to the mean or average and has units matching E. Any general function of E, $h(E)$ can be converted to this form through the normalization in (36).

Reactivity using $<E_{avg}>$ is a linear transformation from that of $<E>$ as shown in (38) and (39). However, the temperature derivative of the reactivity, f, using $<E_{avg}>$ is more complicated. Equation (21) begins the development of that derivative:

$$f' = \frac{df}{dT} = \frac{d(T^{-3/2}\int_0^\infty E\sigma(E)\exp(-E/T)\cdot dE))}{dT} = \frac{d\left(T^{-3/2}<E>\right)}{dT}.$$

Substituting $<E_{avg}>$ for $<E>$ according to (38) provides the starting point for f'. The derivative proceeds as follows:

$$f' = \frac{df}{dT} = \frac{d[C/A(T)]\left(T^{-3/2} < E_{avg} >\right)}{dT}$$

$$f' = \left\{-\frac{3}{2}\left(\frac{1}{T}\right)^{\frac{5}{2}} < E_{avg} > + \left(\frac{1}{T}\right)^{3/2}\frac{d(<E_{avg}>)}{dT}\right\}\left(\frac{C}{A(T)}\right) + \left(T^{-3/2} < E_{avg} >\right)\frac{d[C/A(T)]}{dT}$$

$$f' = \left\{-\frac{3}{2}\left(\frac{1}{T}\right)^{\frac{5}{2}} < E_{avg} > + \left(\frac{1}{T}\right)^{3/2}\frac{d(<E_{avg}>)}{dT}\right\}\left(\frac{C}{A(T)}\right) - \frac{CT^{-3/2}<E_{avg}>}{A(T)^2}\frac{d[A(T)]}{dT}$$

$$f' = \left\{-\frac{3}{2}\left(\frac{1}{T}\right)^{\frac{5}{2}} < E_{avg} > + \left(\frac{1}{T}\right)^{3/2}\frac{d(<E_{avg}>)}{dT}\right\}\left(\frac{C}{A(T)}\right) - \frac{CT^{-3/2}<E_{avg}>}{A(T)}\frac{d(\ln(A(T))}{dT} \tag{40}$$

The f'/f ratio is then:

$$\frac{f'}{f} = \frac{\left(\frac{C}{A(T)}\right)\left\{-\frac{3}{2}\left(\frac{1}{T}\right)^{\frac{5}{2}}<E_{avg}>+\left(\frac{1}{T}\right)^{3/2}\frac{d(<E_{avg}>)}{dT} - T^{-3/2}<E_{avg}>\frac{d(\ln(A(T))}{dT}\right\}}{\frac{C}{A(T)}\left(\frac{1}{T}\right)^{3/2}<E_{avg}>}$$

$$\frac{f'}{f} = -\frac{3}{2}\left(\frac{1}{T}\right) + \frac{d[\ln(<E_{avg}>)]}{dT} - \frac{d(\ln(A(T))}{dT}. \tag{41}$$

Comparing (41) to the first moment ratio in (24):

$$\frac{f\prime}{f} = -\frac{3}{2}\left(\frac{1}{T}\right) + \frac{d(<E>)}{dT}\frac{d[\ln(<E>)]}{d<E>} = -\frac{3}{2T} + \frac{d[\ln(<E>)]}{dT}$$

indicates the same two logarithmic derivative terms in common. There is an additional term in (41) involving the functional relationship of the normalization factor, $A(T)$, with T. This comparison is examined in the Application section below. In summary, Case 2 examines the condition where the first moment, $<E>$, is the average or mean of E, $<E_{avg}>$.

As with $<E_{avg}>$, the estimator introduced in Case 3 has units of energy, keV, but deviates from a strict first moment definition and from the mean, $<E_{avg}>$.

Case 3: Introduction of <*K*> [12]

From the Introduction section, reactivity, f, is defined in terms of E and its general first moment of energy, $<E>$, in (16) as:

$$\int_0^\infty \sigma(E)E\exp\left(\frac{-E}{T}\right)dE = \int_0^\infty E\,h(E)\,dE =< E > \quad ,$$

and in Case 2, the average of E, $<E_{avg}>$ is defined in (38) as:

$$< E_{avg} >= A(T) < E >$$

where $\frac{1}{A(T)} = \int_0^\infty \sigma(E)\exp\left(\frac{-E}{T}\right)dE$ is the normalizing factor for a given T.

In (17), $h(E)$ is assigned as $h(E) = \sigma(E)\exp\left(\frac{-E}{T}\right)$, where cross-section is defined as a function of E. There is a brief discussion of some useful functions for cross-sections in terms of E in the Application section below.

In a classic reference [12], Brysk defines reactivity[2] in terms of relative kinetic energy, K, corresponding to (9):

$$f =< \sigma v >= \left(\frac{m_1+m_2}{\pi m_1 m_2}\right)^{1/2}\left(\frac{T}{2}\right)^{-3/2}\int_0^\infty KdK\sigma(K)\exp\left(\frac{-K}{T}\right) \quad . \quad (42)$$

Brysk defined $<E>$ as the total mean energy of the reaction where $<C>$ is the mean center-of-mass kinetic energy, (different from the constant C used above) and $<K>$ is a ratio[3]:

[2] Brysk's equation (16) in [12].

[3] Brysk's equation (22) in [12].

$$< E >= \frac{<\sigma v(C+K)>}{<\sigma v>} =< C > +< K >$$

$$< C >\equiv 1.5T$$

$$< K >\equiv \frac{<\sigma vK>}{<\sigma v>} = \frac{\int_0^\infty K^2 dK\sigma(K)\exp\left(\frac{-K}{T}\right)}{\int_0^\infty KdK\sigma(K)\exp\left(\frac{-K}{T}\right)} \quad . \tag{43}$$

Brysk interpreted (43) as the mean relative kinetic energy of the reacting particles weighted by the reaction rate.[4] We recognize <*K*> as the ratio of the second moment to the first moment of the relative kinetic energy.

Without providing the steps, Brysk stated the solution[5] of <*K*>, labeled as $< K_{soln} >$:

$$< K_{soln} >= T^2 \frac{d[\ln(T^{1.5}<\sigma v>)]}{dT} = T^2 \frac{d[\ln(T^{1.5}f)]}{dT} \tag{44}$$

Inserting (42), Brysk's function *f*, into his solution in (44), produces the following:

$$< K_{soln} >= T^2 \frac{d\left[\ln\left(T^{1.5}T^{-\frac{3}{2}}\int_0^\infty KdK\sigma(K)\exp\left(\frac{-K}{T}\right)\right)\right]}{dT}$$

$$< K_{soln} >= T^2 \frac{d[\ln(\int_0^\infty KdK\sigma(K)\exp(\frac{-K}{T}))]}{dT} \quad . \tag{45}$$

Examining the derivative of the ln term in <K_{soln}> (44), the following relationships hold:

$$\frac{1}{T^{1.5}f} = \frac{d[\ln(T^{1.5}f)]}{[1.5T^{0.5}f+T^{1.5}f']dT} = \frac{d[\ln(T^{1.5}f)]}{dT}\left(\frac{1}{1.5T^{0.5}f+T^{1.5}f'}\right)$$
$$\frac{d[\ln(T^{1.5}f)]}{dT} = \frac{1.5T^{0.5}f+T^{1.5}f'}{T^{1.5}f} \quad . \tag{46}$$

Inserting the expression in (46) into (44), <K_{soln}> is also:

$$\frac{<K_{soln}>}{T^2} = \frac{1.5T^{0.5}f+T^{1.5}f'}{T^{1.5}f} = 1.5T^{-1} + \frac{f'}{f}$$
$$< K_{soln} >= 1.5T + T^2\frac{f'}{f}. \tag{47}$$

Rearranging (47) shows the $\frac{f'}{f}$ ratio taking on a familiar form:

[4] According to discussion around Brysk's equation (17) in [12].

[5] Brysk's equation (24) in [12].

$$\frac{f'}{f} = -\frac{1.5}{T} + \frac{<K_{soln}>}{T^2}. \quad (48)$$

The $\frac{f'}{f}$ ratio back in (22) is a function of the first moment <*E*>:

$$\frac{f\prime}{f} = -\frac{3}{2}\left(\frac{1}{T}\right) + \frac{d[\ln(T^{1.5}f)]}{dT} = -\frac{1.5}{T} + \frac{d[\ln(C<E>)]}{dT} \quad .$$

Equating the two $\frac{f'}{f}$ ratios from (22) and (48) shows that

$$< K_{soln} > = T^2 \frac{d[\ln\,(C<E>)]}{dT} \quad . \quad (49)$$

Therefore, the solution defined by Brysk, <K_{soln}>, is a function of the general first energy moment, <*E*>, as defined back in (22).

Exploring the relationships between <K_{soln}> and the first energy moment, <*E*>, and between <K_{soln}> and <E_{avg}>, the begs the question of under what conditions are <K_{soln}> and <*E*> the same, and when are <K_{soln}> and <E_{avg}> the same? Recall that <*E*> and <E_{avg}> can be defined in terms of reactivity, *f*, from (21):

$$f = \left(\frac{8}{\pi m}\right)^{1/2}\left(\frac{1}{T}\right)^{3/2} < E > = C\left(\frac{1}{T}\right)^{3/2} < E >$$

$$< E >= \frac{T^{3/2}f}{C},$$

and from (39):

$$< E_{avg} >= \frac{A(T)T^{3/2}f}{C} \quad .$$

Using (47), <K_{soln}> is equal to the first moment <*E*>, when:

$$1.5T + T^2 f'/f = T^{3/2}f/C$$

$$T^2\frac{f'}{f} = \frac{T^{3/2}f}{C} - 1.5T$$

$$\frac{f'}{f} = \frac{T^{3/2}f}{T^2C} - \frac{1.5T}{T^2} = -\frac{1.5}{T} + \frac{f}{T^{1/2}C}$$

$$\frac{f'}{f} + \frac{1.5}{T} = \frac{f}{T^{1/2}C} \quad , \quad (50)$$

and <K_{soln}> is equal to <E_{avg}>, when:

$$\frac{f'}{f} + \frac{1.5}{T} = \frac{A(T)f}{T^{1/2}C} \ . \tag{51}$$

These conditions are examined in the Application section which follows. The relationship between Brysk's ratio of moments definition of $<K>$ in (43) and the solution, $<K_{soln}>$ in (48)-(49), is explored in another paper, planned as Part II of this paper.

IV. Application for D-T Reactivity

A. Cross-Section Discussion

Fusion cross-sections as a function of energy E are have been experimentally measured using nuclear physics instrumentation. For example, a discussion of several different data sets considered for evaluation is in Bosch & Hale [1]. The experiments typically involve accelerating deuterium, and using a tritium target. For this reason, the experimental D+T cross-section data is usually reported in terms of the deuteron lab energy, while the tritium is typically a fixed laboratory target (velocity zero). Under the conditions of an accelerated beam of deuteron incident on a fixed target of tritium, velocity is considered constant, defined by the accelerator energy. The differential fusion cross-section is measured as defined by the (quasi-mono-energetic) deuteron bombarding energy. The D-T fusion cross-section is a charged particle resonance phenomenon. The cross-section experimental data obtained in the laboratory is then analyzed. The data are said to be reduced through evaluation procedures. Over the years, the *published* results for reactivity may be different even though the cross-section sets considered for evaluation, the raw data, may be largely the same. This is to say that reactivity formalisms depend on the data as well as on various authors' procedures and assumptions. There is also a tendency for experimentalists to normalize a data set on resonance. Experimentalists measuring D-T fusion have almost always measured data on the peak of the fusion resonance, because the cross-section is largest there, and the experiments can become easier when the cross-section is large. Experiments at energies below the resonance are typically the most challenging, because cross-sections are low and stopping powers are high. A lack of data at energies below the resonance leaves fitting procedures unconstrained. This was the case for the Duane parametrization, [1].

Some examples of commonly cited reactivity formalisms using various sets of experimental data are [1], [2], and [3]. An example of the procedure for generating values for reactivity as a function of temperature, for Bosch & Hale [1] is given in Hale & Talley [14]:

> "The procedure for generating thermalized TN data [starting from cross-section data] is generally the following:
> One does an analysis of experimental data for the compound system containing the reaction(s) of interest, using the R-matrix code EDA [Energy Dependent Analysis Code, Dodder *et. al.*]. From the minimum-χ^2 solution found by EDA, integrated reaction cross sections are produced on any desired energy grid over the range of the analysis, and written in ENDF format using the code ENDFOR. For reactions leading to three-body final states, the codes SPECT and CMSPECT are used to produce the c.m. [center-of-mass] spectral

moments in ENDF format, as described above. The ENDF-formatted file containing all this information is then fed into STEEPM, which calculates the $<\sigma v>$'s, average energies, and laboratory energy spectra for all outgoing particles."

Multi-channel R-Matrix theory overcomes problems inherent in cross-section parametrizations by putting two-body wave functions into channel radii explicitly. The method incorporates the Coulomb and angular momentum barrier penetration effects at all energies [1]. Nonetheless, less-sophisticated formalisms [2] and [3] describe the resonance region well. Differences can occur off-resonance.

Formalisms [1] [2] [3] are compared below. We believe that an original component of this research is the comparison of the results between evaluations [1] versus [2] and [3], which the authors have not found in any other publication to date. Reference [1] includes comparisons between Bosch and Hale, versus Duane, Peres, and Hively, who are other published authors in the scientific field of D+T fusion. The work of Hively and Peres is referenced in [1].

Figure 1 shows the deuterium-tritium (D-T) cross-section data (barns), over a wide range of deuteron bombarding energy E_d keV) with a maximum around 107 keV. Cross-section is 1.0 barn at about 45 keV and 360 keV. The 625 values, compiled from the Brookhaven National Lab Data Center data base [15], have a mean of 1.33 barns.

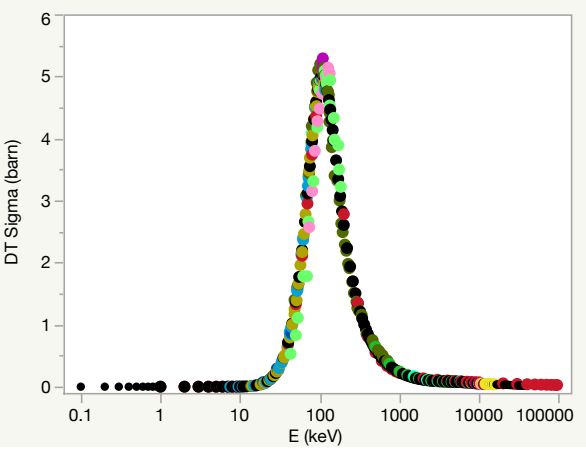

Figure 1: D-T cross-section data from 17 (color-coded) researchers [15] with incident deuteron energy, E_d in keV.

A classic calculation for cross-section comes from Miley et al. [3][6] which cites the Duane [16] formulation as the original source. See also the NRL formulary, Huba [4, p. 44]. Duane's cross-section in the lab frame, with the deuteron accelerated and a stationary tritium target is:

[6]It is interesting to note that Miley, Towner and Ivich chose to display a normalizing ratio, f/T^2, to give the reactivity a smoother shape.

$$\sigma(E) = \frac{\frac{A2}{[1+(A4-A3E)^2]}+A5}{E(\exp(\frac{A1}{\sqrt{E}})-1)} \quad , \tag{52}$$

and the coefficients for D-T are:

$A1 = 45.95$ (keV)$^{1/2}$
$A2 = 50200$ (keV ·barn)
$A3 = 0.01368$ (keV)$^{-1}$
$A4 = 1.076$
$A5 = 409$ (keV ·barn).

In equation (52), the energy denotes the lab energy of the experiments. For deuterons, mass m_d=1875.6 MeV, striking a tritium target, mass m_t=2808.9 MeV at rest, the relation $E_d = \frac{E(m_d+m_t)}{m_t}$ suffices to transform the cross section into center of mass. While not shown in Figure 1, cross-sections using (52) are indistinguishable from those shown over the E range of the measured data. As shown in Bosch & Hale [1, Figure 4], the Duane estimation has the greatest error at low energies, below about 20 keV in the center-of-mass frame where extrapolations of the data are involved.

Classic astrophysics references, *e.g.* [17-18] formulate $\sigma(E)$ for low-energy fusion in terms of the astrophysical factor, $S(E)$. Cross-section can be defined as:

$$\sigma(E) = \frac{S(E)}{E}\exp(-\sqrt{E_C/E}) \tag{53}$$

where E_C is the energy[7] characterizing the magnitude of the Coulomb barrier[8]. The cross-section in (53) can also be expressed in terms of the peak Gamow energy, E_G (found in other literature to be designated E_0)*:*

$$E_G = \left(\frac{T}{2}\sqrt{E_C}\right)^{2/3}. \tag{54}$$

Likewise, there are various formulations for $S(E)$, such as in [11],

$$S(E) = A\exp(-Eb) \tag{55}$$

where A and b is are constants depending upon the reaction[9].

Regardless of the formulations selected, $\sigma(E)$ is analytically tied to E, but not necessarily

---

[7] Other notation is found in the literature, *e.g.* E_G and E_0 may be used for E_C and E_G. Bosch and Hale [1] use B_G for the square-root of E_C.

[8] Given by $E_C = \frac{2\pi^2\mu Z_1^2 Z_2^2 e^4}{\hbar^2}$ which has the value of 1182 keV for the D-T reaction. Bosch and Hale [1] use $B_G = \sqrt{E_C}$ = 34.3827 for $D(t,n)^4_4He$; B_G = 68.7508 for $^3_4He(d,p)^4_4He$; B_G = 31.3970 for $D(d,p)T$; and B_G = 31.3970 for $D(d,n)^3_4He$, units of $\sqrt{keV}$.

[9] $A = 9821$ barns · keV, $b = -0.029$ keV^{-1} for the D-T reaction, Kaye and Laby [11].

to *T*. Because of the former, the cross-section cannot be extracted from the integral, and because of the latter, it is unaffected by taking the temperature derivative.

Inserting the astrophysics-based cross-section (53) into reactivity (18) gives

$$\begin{gathered} f = T^{-3/2}\int_0^\infty \sigma(E)\cdot E\cdot \exp(-E/T)dE \\ f = T^{-3/2}\int_0^\infty \frac{S(E)}{E}\exp\left(-\sqrt{E_C/E}\right)E\exp(-E/T)dE. \\ f = T^{-3/2}\int_0^\infty S(E)\exp(-E/T-\sqrt{E_C/E})dE \end{gathered} \tag{56}$$

Then applying (55), which relies on Kaye & Laby [11], gives an integrand in terms of three exponentials.

$$f = AT^{-3/2}\int_0^\infty \exp(-Eb-E/T-\sqrt{E_C/E})dE \quad . \tag{57}$$

With known values of *E*, *b* and E_C, the reactivity in (57) could be solved numerically.

It is customary in the astrophysics literature [17-18], to compare the exponential terms in (54-56). Of note is that the right tail of the MB distribution occurs at lower energies than these other exponential effects. Also of note is that *S*(*E*) belies the broad D-T resonance, a varying function, positioned at higher energies relative to MB. Bosch & Hale's Figure 2 [1, p. 614] shows that the *S*(*E*) function peaks at about 48 keV, with the Gamow peak in between.

While other expressions for cross-section can be found in the literature, it is not the purpose here to provide a complete listing.

B. First Moment D-T Reactivity

Three different reactivity formulations [1], [2], and [3] are presented to demonstrate the first energy moment and reactivity temperature derivative relationships developed herein. Note that all three of these are developed to accommodate cross-section varying with energy.

1. The Bosch & Hale (B&H) [1] reactivity, *f*, and first derivative with *T*, f', are given by the formulas below. The constants can be found in [1].

$$f = C_1\theta\sqrt{\xi/(mc^2T^3)}\exp(-3\xi) \tag{58}$$

where

$$\theta = T/\left(1-\frac{(C_2T+C_4T^2+C_6T^3)}{(1+C_3T+C_5T^2+C_7T^3)}\right) \text{ and } \xi = \frac{{B_G}^2}{(4\theta)^{1/3}} \ ,$$

and

$$f' = \frac{-5f}{6\theta}\frac{d\theta}{dT} - \frac{2f}{3T} + \frac{f}{T}\left[\frac{-C_1T^{2/3}}{\theta^{2/3}}\frac{d\theta}{dT} - \xi\theta^{1/3}\right] \tag{59}$$

where

$$\frac{d\theta}{dT} = \frac{-[(\theta-1)(C_3+2C_5T+3C_7T^2)+(C_2+2C_4T+3C_6T^2)]}{(1+C_3T+C_5T^2+C_7T^3)} \text{ and } \frac{d\xi}{dT} = \frac{-\xi}{3T}.$$

2. The Caughlan & Fowler (C&F) original formulation [2] is given as a reaction rate (*RR*):

$$RR = N_A f(T9) \tag{60}$$

where N_A is Avogadro's number, and where temperature $T9$ is in units of a billion degrees Kelvin. This *RR* parameterization and the use of $T9$ are the convention for stellar nucleosynthesis.

$$f(T9) = \frac{1B_0/\mathrm{T9}^{2/3}\exp(B_1/\ \mathrm{T9}^{1/3}-\{\mathrm{T9}/B_2\}^2)\cdot[1.0+B_3\mathrm{T9}^{1/3}+B_4\mathrm{T9}^{2/3}+B_5\mathrm{T9}+B_6\mathrm{T9}^{4/3}+B_7\mathrm{T9}^{5/3}]}{N_A} + \frac{B_8/\mathrm{T9}^{2/3}\exp(B_9/\mathrm{T9})}{N_A} \tag{61}$$

For the D-T fusion reaction, the parameters are:

$B_0 = 8.09\text{x}10^{10}$,
$B_1 = -4.524$,
$B_2 = 0.120$,
$B_3 = 0.092$,
$B_4 = 1.80$,
$B_5 = 1.16$,
$B_6 = 10.52$,
$B_7 = 17.24$,
$B_8 = 8.73\text{x}10^{8}$,
$B_9 = -0.523$.

The conversion between $T9$ and T(keV) is $T9=0.0116T$. [10]

The first derivative of the reaction rate, *RR* (60) with $T9$ is:

$$\frac{dRR}{dT9} = -\frac{B_8B_9exp(B_9/T)}{T^{8/3}} - \frac{2RR}{3T} + \frac{B_0exp(B_1/T^{1/3}-T^2/B_2T^2)(\frac{B_3}{3T^{2/3}}+\frac{2B_4}{3T^{1/3}}+B_5+\frac{4}{3}B_6T^{1/3}+\frac{5}{3}B_7T^{2/3})}{T^{2/3}} + \frac{B_0exp(B_1/T^{1/3}-T^2/B_2T^2)(-B_1/3T^{4/3}-2T/B_2{}^2)(1+B_3T^{1/3}+B_4T^{2/3}+B_5T+B_6T^{4/3}+B_7T^{5/3})}{T^{2/3}} \tag{62}$$

To calculate df/dT from dRR/d$T9$ requires the following transformation and use of the chain rule

[10] 1 electron volt = 11600 degrees Kelvin, T9 = 86.17 keV.

$$\frac{1}{N_A}\frac{df}{dT9} = \frac{dRR}{dT9}$$

and

$$f' = \frac{dT9}{dT} \cdot \frac{df}{dT9} \tag{63}$$

where d$T9$/dT=0.0116. Thus, the analytical derivative in (62) is divided by N_A and multiplied by 0.01106.

3. Miley, Towner, and Ivich (MTI) [3] tabulated D-T reactivity values for a T range from 1-1000 keV. For T<25, these were fitted to a function appearing in NRL Plasma Formulary, Huba [4]:

$$f(T) = A_0 T^{-2/3} \exp(-AT^{-1/3}) \tag{64}$$

where A=19.94 and A_0=3.68 x 10^{-12}. The first derivative of reactivity with temperature is:

$$\frac{df}{dT} = f' = \frac{A_0(A-2T^{1/3})\exp(-AT^{-1/3})}{3T^2}. \tag{65}$$

See also Langenbrunner & Makaruk [5] and Langenbrunner & Booker [7]. However, for the table of values over the full range of T, the first derivative can be approximated using finite differencing:

$$df(T_i)/dT=0.5[f(T_i)-f(T_{i-1})/(T_i-T_{i-1})]+0.5[f(T_{i+1})-f(T_i)/(T_{i+1}-T_i). \tag{66}$$

4. Comparing the Three Reactivity Evaluations

Figure 2 shows the three reactivity formulations, and Figure 3 shows their first T derivatives with the log(T) scale.

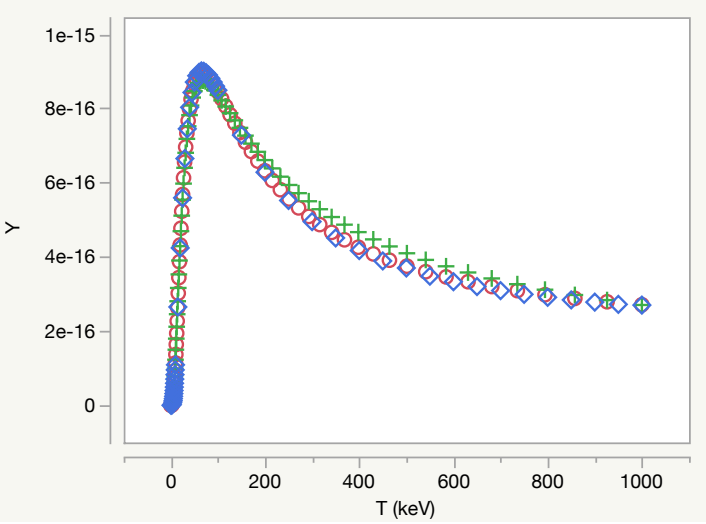

Figure 2. D-T reactivity, *f*, plots for 3 formulations: B&H (red), C&F (green) and MTI (blue).

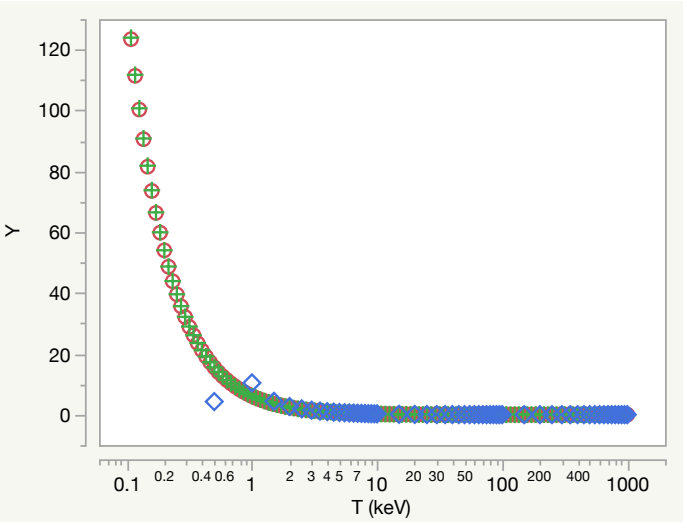

Figure 3. D-T reactivity first *T* derivative, f'/f, B&H (red), C&F (green), and MTI (blue) on the log(*T*) scale. The 2 blue diamonds appear out of alignment because they are the starting values for the finite differencing used to determine the derivative.

A closer examination of the Figure 3 derivatives in Figure 4 reveals a crossing of the zero axis near $T = 64$ keV for all three formulations.

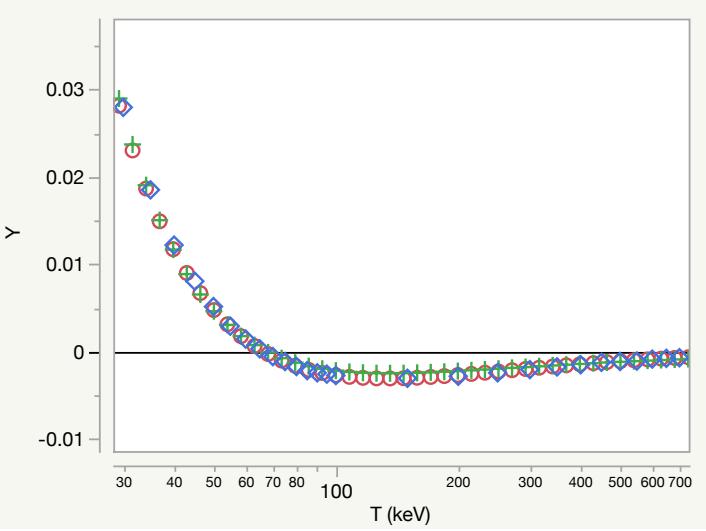

Figure 4. Expansion of the plotting scale, for the D-T reactivity first *T* derivative, f'/f, B&H (red), C&F (green) and MTI (blue) on the log(*T*) scale. The crossing at 64 keV is expected, because that is the peak of the resonant D-T fusion cross-section.

Table I contains selected values of the f'/f ratio for the three reactivity formulations

displayed in Figures 3 and 4.

TABLE I Selected Values of D-T f'/f Comparing B&H, C&F and MTI.

T (keV)	MTI f'/f	C&F f'/f	B&H f'/f
0.5	4.30	15.53	15.52
1	10.44	6.09	6.10
2	2.67	2.39	2.24
5	0.72	0.75	0.71
10	0.27	0.27	0.25
20	0.069	0.060	0.068
50	0.0052	0.0047	0.0046
100	-0.0027	-0.0022	-0.0027
200	-0.0028	-0.0022	-0.0027
500	-0.0011	-0.0011	-0.0011
800	-0.0005	-0.0008	-0.0006
1000	-0.0001	-0.0006	-0.0004

In Table I, f'/f columns for B&H, C&F and MTI are seen to be very close as indicated by Figures 2 and 3.

5. Comparing Constant and Varying Cross-Sections

The f'/f values from B&H, C&F and MTI reactivities and reactivity derivatives are based upon varying, evaluated, D-T fusion cross-sections. Therefore, these reactivities are not appropriate for the constant cross-section special case, $<E^*>$, or its $f^{*\prime}/f^*$ ratio in (34),

$$\frac{f^{*\prime}}{f^*} = \frac{\left(-\frac{1}{2}\left(\frac{1}{T}\right)^{3/2}<E^*>+\left(\frac{1}{T}\right)^{5/2}<E^*>^2\right)}{\left(\frac{1}{T}\right)^{\frac{1}{2}}<E^*>} = \frac{-1}{2T}+\frac{<E^*>}{T^2} \ .$$

Calculations for the constant cross-section case are determined from their T-based expressions. Recall that $<E^*>$ is the mean of the exponential pdf which is T from (31). The reactivity, T derivative, and $f^{*\prime}/f^*$ ratio are determined using equations (31), (32) and (33):

$$< E^* >= T$$

$$f^* = \left(\frac{8}{\pi m}\right)^{1/2}\left(\frac{1}{T}\right)^{\frac{1}{2}}\sigma < E^* > = C\left(\frac{1}{T}\right)^{\frac{1}{2}}\sigma < E^* > = C\sigma T^{1/2}$$

$$\frac{f^{*\prime}}{C\sigma} = T^{-5/2} < E^* >^2 - 0.5 < E^* > T^{-\frac{3}{2}}$$

$$f^{*\prime} = C\sigma\left\{T^{-5/2}T^2 - 0.5TT^{-\frac{3}{2}}\right\} = C\sigma 0.5\left(\frac{1}{T}\right)^{1/2} \quad .$$

Therefore, the $f^{*\prime}/f^*$ ratio is calculated as:

$$\frac{f^{*\prime}}{f^*} = \frac{C\sigma 0.5\left(\frac{1}{T}\right)^{1/2}}{C\sigma T^{1/2}} = 0.5/T \quad . \tag{67}$$

Case 3 is the development of the expression for Brysk's solution, $<K_{soln}>$, in terms of the f'/f ratio in (47):

$$\frac{f'}{f} = -\frac{1.5}{T} + \frac{<K_{soln}>}{T^2}$$

$$< K_{soln} >= T^2\frac{f\prime}{f} + \frac{3T}{2} \quad .$$

Figure 5 compares $<K_{soln}>$ (varying cross-section) using (47) and the B&H reactivity f'/f values with $<E^*>$ (constant cross-section). The (blue) line is $< E^*> = T$. The nonlinear $<K_{soln}>$ (red) wraps around the constant cross-section line. In spite of the linear versus nonlinear differences, $< E^*>$ does not appear that different from $<K_{soln}>$ (varying cross-section). That impression changes in subsequent comparisons.

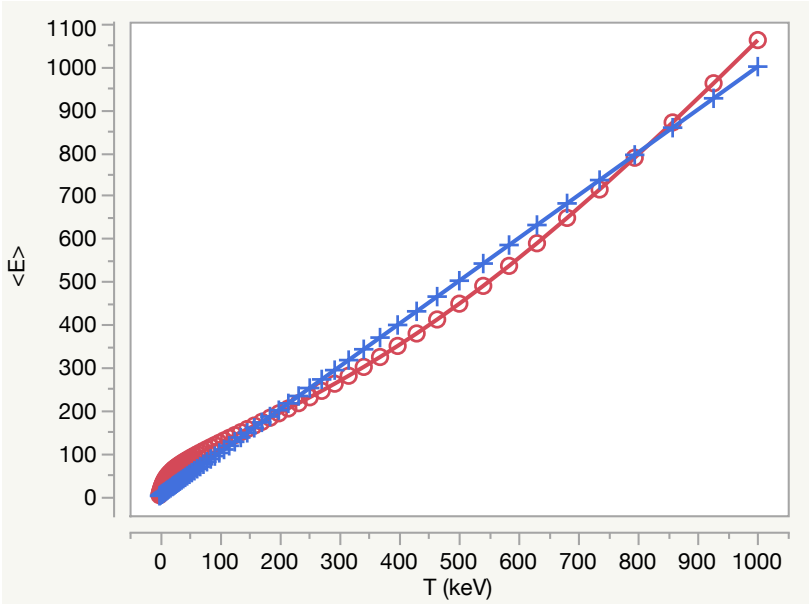

Figure 5. $<K_{soln}>$ using f'/f from B&H (red) and $< E^*>$ (blue).

Figure 6 compares the reactivities for varying cross-section, f, using the B&H formulation (58) and for constant cross-section, f^* in (27). To calculate the latter requires determining a value for constant cross-section, σ, then values for each T. For purposes of illustration only, those cross-sections were determined using the peak Gamow energy, from (54), $E_G = \left(\frac{T}{2}\sqrt{E_C}\right)^{2/3}$. The Duane cross-sections (52) were then determined for those E_G values. For the D-T reaction, $\sqrt{E_C}$=34.38,[11] and the leading constant from the coefficients is 1.1284e+12.

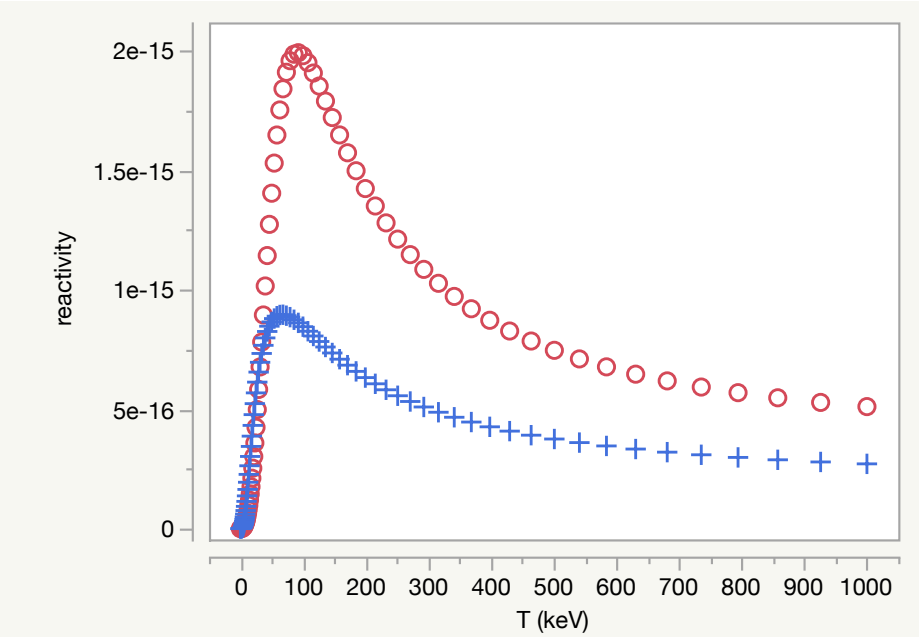

Figure 6. B&H reactivity, f (blue), and f^* (red) using Duane constant cross-section at peak Gamow, E_G.

The maxima for f and f^* are very different—64 and 136 keV, respectively. The maxima for f is 64 keV because the fusion resonance peaks at 64 keV in the center of mass, (deuteron bombarding energy 107 keV in the lab frame.) The higher f^*curve is not surprising because the Gamow energies are larger than T for T<300 keV.

Figure 7 shows the nonlinear relationship between E_G, and T. One might be tempted to conclude that the differences between these two reactivity curves is due to the choice of E values. Other choices were examined without improving the alignment of the reactivity

[11] B_G in the notation of Bosch & Hale [1].

curves. The conclusion is that reactivity curve differences are due to the difference between constant cross-section and varying resonant cross-section.

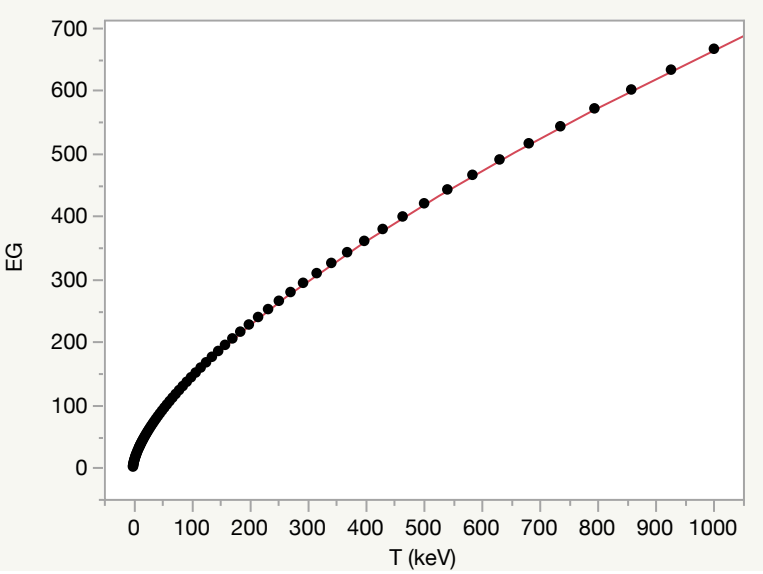

Figure 7. Gamow peak, E_G, and T.

Figure 8 compares the reactivity first T derivatives of varying versus constant cross-sections, f' and f'^*, respectively. Here there are significant differences. The varying-cross-section reactivity derivative (red) crosses the horizontal axis, going negative near T=64 keV. In contrast the constant cross-section reactivity derivative curve (blue) remains positive.

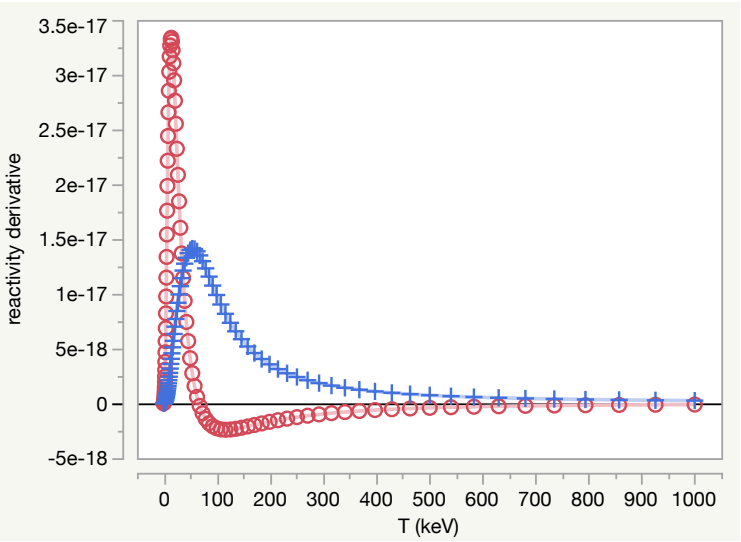

Figure 8. Reactivity T derivatives: f' (red) and f'^* (blue).

Figure 9 compares the f'/f and f'^*/f ratios on log(T) scale. The constant cross-section ratio is confined to values between 5.0 and 0.0005, whereas the B&H ratios range as large

as 137 at the lower temperatures. As shown in Figure 4, the B&H ratios cross into negative values at T=64 keV, but the constant cross-section ratios remain positive.

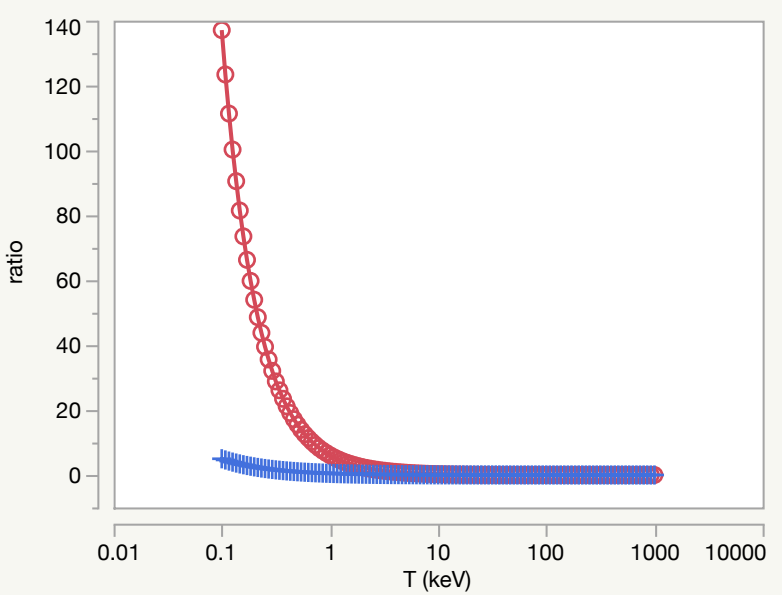

Figure 9. Reactivity ratios: f'/f (red) from B&H and f'^*/f (blue) on log(T) scale.

Figure 10 focuses in on the T region where f'/f (red) from B&H crosses into negative values.

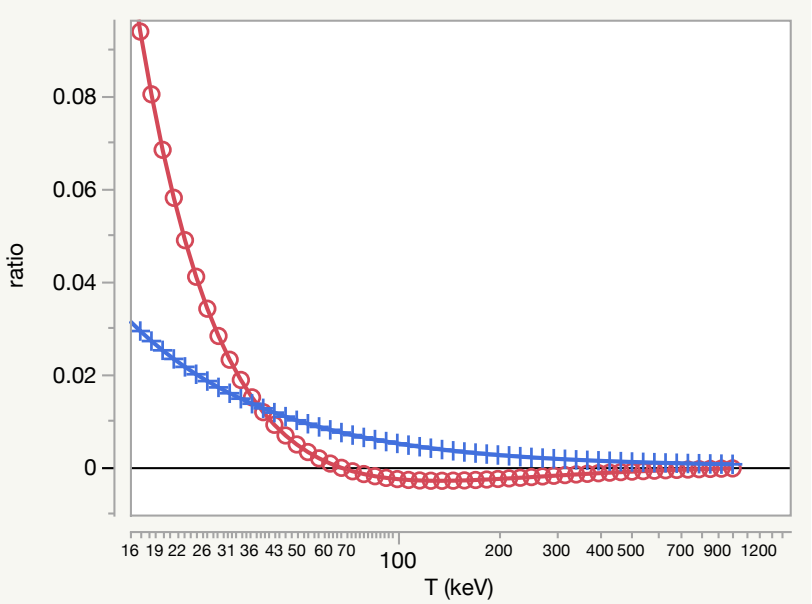

Figure 10. Close-up of ratios: f'/f from B&H (red) and f'^*/f (blue) on log(T) scale.

These significant differences between the constant and varying cross-sections illustrated in

Figures 5-10 make the case for the importance of varying cross-sections, in spite of the analytical difficulties that imposes. These figures demonstrate that the convenience of assuming constant cross-sections alters the story of reactivity behavior. This is especially noticeable with the changes of shapes for the reactivity derivative and the f'/f ratio. As demonstrated in other papers in this study, those quantities relate to other observables, such as flux and reaction history from inertial confinement fusion experiments in [8].

6. Least Square Fits

Comparing equations (34):

$$\frac{f^{*\prime}}{f^*} = \frac{-1}{2T} + \frac{<E^*>}{T^2}$$

and (48):

$$\frac{f\prime}{f} = -\frac{3}{2T} + \frac{<K_{soln}>}{T^2},$$

their forms are similar, as functions of the f'/f ratios. That form can be generally expressed as a linear model for a generic first moment energy estimator, <*E*>,

$$\frac{f\prime}{f} = b_0 + b_1\frac{1}{T} + b_2\frac{<E>}{T^2} \quad . \tag{68}$$

For a given set of <*E*> values, the coefficients matching those in (34) for <E^*> would not be significantly different from:

$$b_0 = 0,\ b_1 = -0.5,\ b_2 = 1.0,$$

and the coefficients matching those in (48) for <K_{soln}> would not be significantly different from:

$$b_0 = 0,\ b_1 = -1.5,\ b_2 = 1.0.$$

The left side of (68), the reactivities, can be determined from the three evaluations: B&H, C&F and MTI. For a given set of <*E*> values at values of *T,* least squares fits provide the estimates of the coefficients in (68).

Hale [14] provided a set of <*E*> values[12], and these were used in the least squares fits in (68) with f'/f values from B&H and C&F[13] to determine the coefficients. Figure 11 shows Hale's set. Some values are in Table I.

[12] Gerry Hale (Los Alamos National Laboratory) provided 121 calculated <*E*> values covering a *T* range of 0.20-1000.0 keV.

[13] There were too few tabled values for MTI fits.

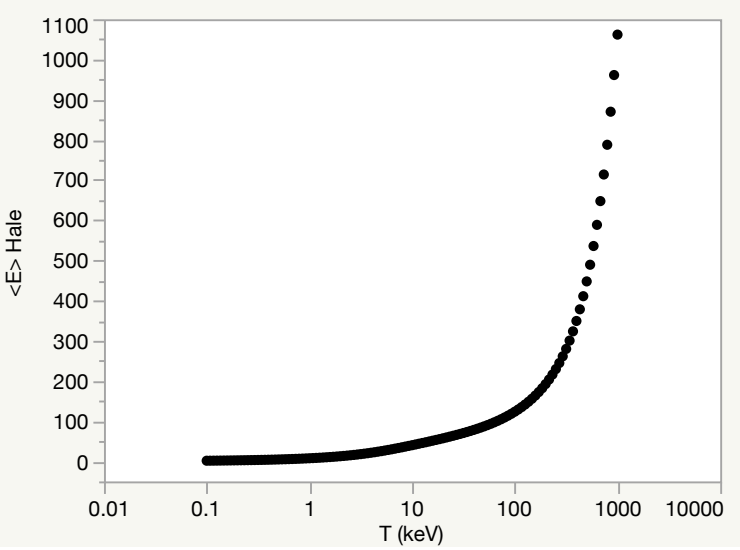

Figure 11. Calculated <*E*> values provided by G. Hale [14] verses *T*.

The B&H and C&F fits indicated that b_0 was not (statistically) different from zero, and b_2 was 1.0, as expected from (34).

The B&H ratio was fit to the Hale[14] <*E*> values, resulting in $b_1 = -1.54$. At first glance, it appears that -1.54 should be close enough to the value -1.50, the value corresponding to Brysk's solution (48). Statistically, the fit with Hale <*E*> value is significantly different from -1.50. The reason for this is due to the nearly perfect match of Hale's <*E*> values using the B&H reactivities. The error in the fitting is so small that a parameter difference of 0.04 is significantly different at the 5% level of significance. This could be considered a case where *practical* significance overrides *statistical* significance, resulting in the conclusion that Hale's values follow Brysk's solution. The Hale <*E*> values are thus verified to belong to the Bosch and Hale formalism. Moreover, the fitting function in (68) is justified.

The C&F ratio was fit to the Hale <*E*> values, resulting in b_1=-1.58, which is significantly different from Brysk's solution (48), $b_1 = -1.50$. This difference in b_1 is more pronounced, retaining the statistical conclusion regarding a difference.

Thus, neither the B&H the C&F values are statistically consistent with the $\langle K_{soln} \rangle$ expression. Neither B&H nor C&F are consistent with the expected value of -0.5 from (34), the $\langle E^* \rangle$ definition. That is not surprising because the f'/f values ratios were developed with the energy-varying cross sections.

The results of these least squares fits illustrate that the b_1 coefficient is sensitive to changes in the f'/f values. The goodness of the fits contributes to this sensitivity. The results also confirm that B&H and C&F reactivity formulations are closely related for these *T* ranges—

[14] Gerry Hale (Los Alamos National Laboratory) [14] provided 121 calculated <*E*> values covering a *T* range of 0.20-1000.0 keV.

which was observed in Figures 3 and 4.

Table II contains the energy estimators from the three cases: $<E^*>$, $<E_{avg}>$, and $<K_{soln}>$ for selected values of T. The column $<E^*>$ is the constant cross-section which is calculated as T from (31). The columns with $< K_{soln} >$ from B&H and C&F and are obtained using equation (47):

$$< K_{soln} >= 1.5T + T^2 \frac{f'}{f}.$$

The Hale provided $<E>$ values match those for $<K_{soln}>$ (in (49)) from both B&H up to 50 keV, and from C&F up to 5 keV. The last column is the calculated first moment, the average, $<E_{avg}>$ using (39):

$$f = \frac{C}{A(T)}\left(\frac{1}{T}\right)^{3/2} < E_{avg} >.$$

For the $<E_{avg}>$ entries in Table II, reactivity, f, used equation (58) from Bosch & Hale [1]. The cross-sections for calculating $<E_{avg}>$ were also taken from this work [1]. Implementing (39) requires determination of the normalization factor, $A(T)$ from (38):

$$\frac{1}{A(T)} = \int_0^\infty \sigma(E) \exp\left(\frac{-E}{T}\right) dE.$$

It should be noted that $<E_{avg}>$ values are sensitive to $A(T)$, and that determination was made using finite differencing and summations on a coarse grid for only a few values of T. Therefore, $<E_{avg}>$ values in Table II are only approximate and subject to change using more accurate numerical methods.

TABLE II Selected Values of D-T for the three cases: $<E^*>$, $<E_{avg}>$, and $<K_{soln}>$, units of keV.

T (keV)	Hale [14] $<E>$	$<K_{soln}>$ from B&H	$<K_{soln}>$ from C&F	$<E^*>=T$	$<E_{avg}>$ from (39)
0.5	4.6	4.6	4.7	0.5	4.6
1	7.6	7.6	7.6	1	7.7
2	12.6	12.6	12.5	2	13.0
5	25.3	25.3	26.3	5	25.1
10	40.1	40.0	41.9	10	40.2
20	57.2	57.1	53.8	20	60.9
50	86.9	87.1	86.8	50	108
100	123	123	128	100	160

200	192	193	211	200	242
500	447	482	463	500	502
800	788	838	707	800	819
1000	1062	1112	878	1000	1031

Figure 12 shows the columns in Table II plotted with T, except for $\langle K_{soln} \rangle$ from C&F.

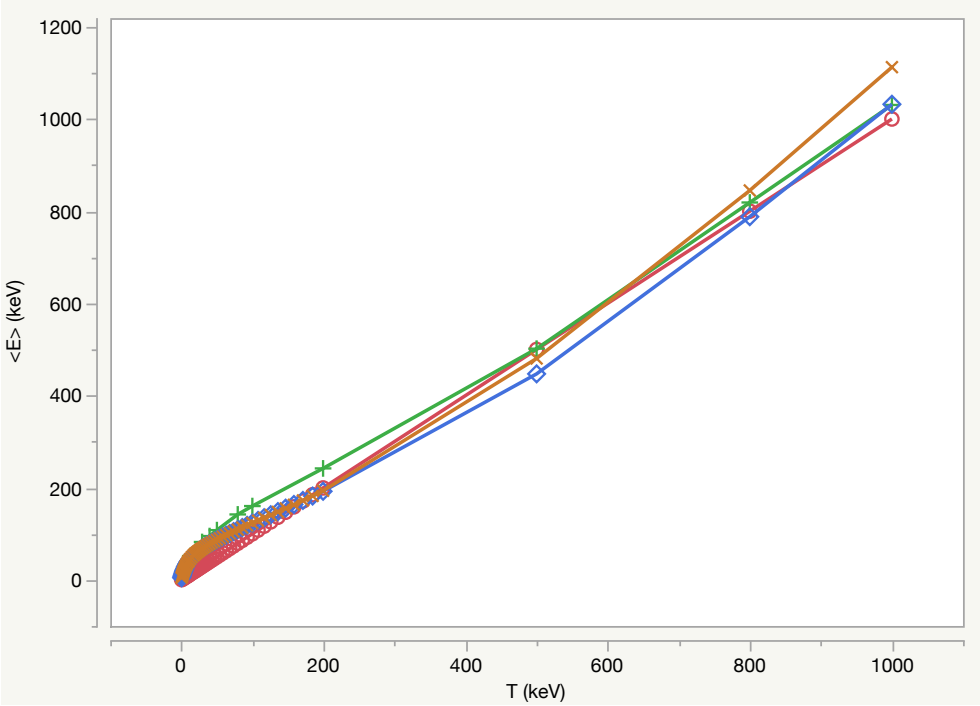

Figure 12. $\langle E^* \rangle$ in red circles, $\langle E_{avg} \rangle$ in green pluses, $\langle E \rangle$ sent from Hale in blue diamonds, and $\langle K_{soln} \rangle$ in gold x's.

At the end of Case 3, equations (50) and (51) established the condition for when $\langle K_{soln} \rangle$ is equal to the first moment $\langle E \rangle$ as

$$\frac{f'}{f} + \frac{1.5}{T} = \frac{f}{T^{1/2}C} \quad ,$$

and when $\langle K_{soln} \rangle$ is equal to $\langle E_{avg} \rangle$ as:

$$\frac{f'}{f} + \frac{1.5}{T} = \frac{A(T)f}{T^{1/2}C} \quad .$$

Using the B&H reactivity for f and f', Figures 13 and 14 show the relationships between the left and right sides of (50) and (51) respectively. In both these figures the left sides of the equivalence condition is plotted against the right sides. The nonlinear relationship shown in Figure 13 indicates the difficulty in establishing the equality between $\langle K_{soln} \rangle$ is

equal to the first moment <E>. The radically different scales of the axes contributes to this difficulty. In Figure 14, the scales of both axes are similar, and the relationship is nearly linear. The slope is significantly different from 1.0, and the intercept is also significantly different from zero, indicating the equivalency is not achieved. However, the possibility for equivalency is more likely for <K_{soln}> with <E_{avg}> than it is with the first moment, <E>.

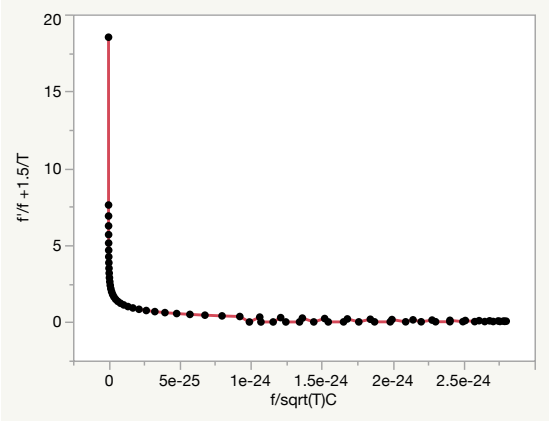

Figure 13. Condition for <K_{soln}> equal to the first moment <E> according to left and right sides of (50).

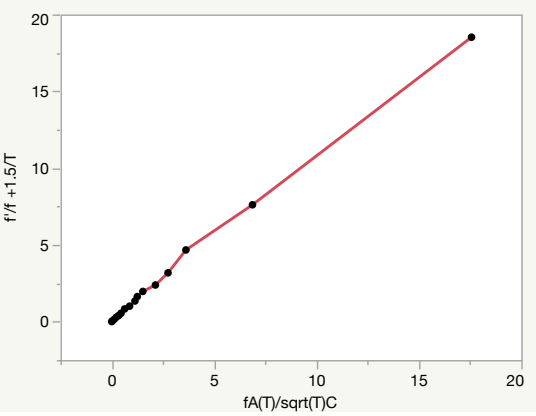

Figure 14. Condition for <K_{soln}> equal to <E_{avg}> according to left and right sides of (51).

V. Summary

Definition for the first moment of kinetic energy is presented in terms of reactivity and its derivative with temperature. One case of that definition was developed assuming constant cross-section, <E^*>, and two cases with varying cross-sections. Case 2 examines the condition where the first moment, <E>, is the average, or mean of E, <E_{avg}>. Case 3 corresponds to a solution given by Brysk [5], <K_{soln}>. The constant cross-section case focuses on the first moment definition, <E>; whereas the varying cross-section cases are based upon a function of that definition. Analytical differences are specified between these cases, and, in each case, analytical expressions are developed in terms of reactivity and its first temperature derivative.

The varying cross-section cases are demonstrated for D-T fusion, indicating their differences using three reactivity formulations from Bosch & Hale [1], Caughlan and Fowler [2], and Miley, Towner, and Ivich [3]. These three are shown to perform similarly, (but with details that could be assessed quantitatively). The differences in reactivities between the constant cross-section and the varying cross-section cases are large relative to differences between the three reactivity formulations. The application of these for D-T fusion confirms the conclusion about differences resulting from assuming a constant cross-section versus the well-known fusion resonance.

The differences between the first moment-based estimators: $\langle E^* \rangle$, $\langle E_{avg} \rangle$ and $\langle K_{soln} \rangle$ vary according to the values of temperature. By definition $\langle E^* \rangle = T$; therefore, nonlinear effects from varying cross-sections are not represented. While $\langle E_{avg} \rangle$ is a normalized version of the first moment, $\langle K_{soln} \rangle$ is a nonlinear function of it. Therefore, differences between them are especially pronounced if consideration is given to the differences in definitions, $\langle E^* \rangle$, $\langle E_{avg} \rangle$ and $\langle K_{soln} \rangle$.

During the process of V&V, uncertainty comprises comparing different, published formulations, B&H to C&G, to MTI. The reactivity formulations, or models, differ, and those differences can represent differences in the measured cross sections accepted for evaluation, and in how the physics is manifest. In addition, uncertainty arises from applying any formulation beyond its established domain of applicability. These three models were developed using a fitting of their mathematical forms to experimental results and/or established calculations. Even though Table I indicates a consistency in reactivities between the three (chosen) formulations, uncertainties in that fitting process and a comparison of other formulations (not chosen, such as Peres [19]) should be included as part of the V&V process. Use of the C&G formulation will be expanded by the authors, because of the many other nuclear reactions in its purview.

The follow-on paper, planned as Part II, continues the analytical development of the moment-based definition used by Brysk [12] and its relationship to the definitions and solutions in Part I. See also Langenbrunner & Booker [20] for examples using numerical values.

References

[1] H.S. Bosch and G.M. Hale "Improved Formulas for Fusion Cross-sections and Thermal Reactivities" *Nuclear Fusion*, Vol. 32 No. 4, 1992, pp. 611-631.

[2] G.R. Caughlan and W.A. Fowler, "Thermonuclear Reaction Rates V", *Atomic and Nuclear Data Tables,* 40, pp. 283-334, Academic Press, 1988, Tables I, II and III.

[3] G.H. Miley, H. Towner, and N. Ivich, "Fusion Cross Sections and Reactivities," University of Illinois, Nuclear Engineering Program, Report C00-2218-17, June 1974, http://ww.osti.gov/sciteh/servlets/purl/4014032

[4] J.D. Huba, NRL Plasma Formulary, Naval Research Laboratory, NRL/PU/6790-040447, Revised 2004. Also see 2019 version, available online.

[5] J.R. Langenbrunner, H. Makaruk, “Temperature Derivatives for Fusion Reactivity of D-D and D-T,” Los Alamos National Laboratory report, LA-UR-16-29065, Jan. 2016.

[6] J.R. Langenbrunner and J.M. Booker, “Analysis on NRL Plasma Formulary D-T Reaction Rate Formula,” Los Alamos National Lab Technical Report, Feb. 14, 2013, LA-UR-13-21233.

[7] J.R. Langenbrunner and J.M. Booker, “Analytic, empirical and delta method temperature derivative of D-D and D-T fusion reactivity formulations, as a means of verification,” Los Alamos National Laboratory Technical Report, LA-UR-17-26143, July, 2017. Available from OSTI.gov, online, https://www.osti.gov/biblio/1372790/.

[8] J.R. Langenbrunner and J.M. Booker, “Chain Rule Approach for Calculating the Time-Derivative of Flux,” Los Alamos National Laboratory, LA-UR-17-21233, Oct. 2017. Available from OSTI.gov online https://www.osti.gov/biblio/1398942/.

[9] J.R. Langenbrunner and J.M. Booker, “Power Index Tables for Burning D-T and D-D Plasma,” Los Alamos National Laboratory, LA-UR-18-22364, March 2018.

[10] Maxwell-Boltzmann Distribution, Wikipedia, https://en.wikipedia.org/wiki/Maxwell–Boltzmann_distribution

[11] G.W.C. Kaye and T.H. Laby Tables of Physical & Chemical Constants, section 4.7.4 Nuclear Fusion, 2005 online. http://www.kayelaby.npl.co.uk/atomic_and_nuclear_physics/4_7/4_7_4.html.

[12] H. Brysk, “Fusion Neutron Energies and Spectra” Plasma Physics, Vol 15, pp. 611-617, 1973.

[13] W.A. Fowler, G.R. Caughlan and B.A. Zimmerman, “Thermonuclear reaction rates II”, Ann. Rev. Astron. Astrophysics, Vol 13, pp. 69-112, 1975. See also Ann. Rev. Astron. Astrophysics, 1967.

[14] G.M. Hale, T.L. Talley, “Maxwellian-Averaged Data for Thermonuclear Reactions,” March 16, 2009. Gerry Hale (Los Alamos National Laboratory) provided 121 calculated $\langle E \rangle$ values covering a T range of 0.20-1000.0 keV . These were made available by private communications with Gerry Hale, Los Alamos National Laboratory, co-author of [1].

[15] Brookhaven National Laboratory Nuclear Data Center—Experimental Nuclear Reaction Data: http://www.nndc.bnl.gov/exfor/exfor.html.

[16] B.H. Duane, "Fusion Cross Section Theory," BNWL-1685 (1972). See also the Naval Research Lab Formulary, 2019, pp. 44, 45, available online.

[17] H. Rogers, “Thermonuclear Burn (U)” Los Alamos National Laboratory viewgraphs, January 26, 2000, Thermonuclear Applications Group.

[18] S. Atzeni and J. Meyer-Ter Vehn, *The Physics of Inertial Fusion: Beam Plasma Interaction, Hydrodyanmics, Hot Dense Matter*, Oxford Science Publications, 2004. Clarendon Press Oxford. Extracted from draft by Stefano Atzeni Chapter 1 2004/4/29 “Nuclear fusion reactions” 2004/4/29, page 17 eqn 1.59. http://www.fisicanucleare.it/documents/0-19-856264-0.pdf

[19] A.J. Peres, “Fusion Cross-sections and Thermonuclear Reaction Rates,” Journal of

Applied Physics, 50, 5569, 1979.

[20] J.R. Langenbrunner, J.M. Booker, “Numerical Examples for Hydrogen Isotope Funsion Reactivity Under the Maxwell-Boltzmann Assumption,” Technical Report, July 30, 2020.

Appendix A
Development of the MB Velocity Distribution

The single species velocity, v_j, distribution known as the Boltzmann distribution or the Maxwell distribution is:

$$f(v_j) = A\exp\left(\frac{-mv_j{}^2}{2kT^\circ}\right). \tag{A1}$$

The leading term, A, is defined so that $\int_{-\infty}^{\infty} f(v_j)\, dv_j = 1$.
Then, imposing the constraint:

$$\int_{-\infty}^{\infty} f(v_j) dv_j = A\int_{-\infty}^{\infty} \exp\left(\frac{-mv_j{}^2}{2kT^\circ}\right) dv_j = 1. \tag{A2}$$

Recognizing that $\int_{-\infty}^{\infty} e^{-x^2}\, dx = \sqrt{\pi}$, define x as

$$x = v_j\left(\frac{m}{2kT^\circ}\right)^{0.5}. \tag{A3}$$

The factor $\left(\frac{m}{2kT^\circ}\right)^{0.5}$ must be included into the integrand for the constraint in (A2) to hold:

$$\int_{-\infty}^{\infty} f(v_j) = A\left(\frac{2kT^\circ}{m}\right)^{0.5}\int_{-\infty}^{\infty}\left(\frac{m}{2kT^\circ}\right)^{0.5}\exp\left(\frac{-mv_j{}^2}{2kT^\circ}\right) dx. \tag{A4}$$

For the integral to be $\sqrt{\pi}$ then A must satisfy the following:

$$\mathrm{A}\left(\frac{2kT^\circ}{m}\right)^{0.5}\sqrt{\pi} = 1$$

$$A = \left(\frac{m}{2\pi kT^\circ}\right)^{0.5}. \tag{A5}$$

Therefore, the single species velocity Boltzmann distribution or the Maxwell distribution is:

$$f(v_j) = \left(\frac{m}{2\pi kT^\circ}\right)^{0.5}\exp\left(\frac{-mv_j{}^2}{2kT^\circ}\right). \tag{A6}$$

Development of the MB Velocity Distribution in 3 Directions

Considering the velocity as comprised of its three directional components, the following definition for v was given in (3):

$$v^2 = v_x{}^2 + v_y{}^2 + v_z{}^2$$
$$v = \sqrt{v_x{}^2 + v_y{}^2 + v_z{}^2}. \tag{3}$$

The Boltzmann single series, one direction, Boltzmann (aka Maxwell) distribution is given above in (A6). Assuming independence between the three directions, the joint distribution $f(v_x v_y v_z)$ is the three-fold product of the single distribution:

$$f(v_x v_y v_z) = f(v_x)f(v_y)f(v_z) = \left(\frac{m}{2\pi kT^\circ}\right)^{3/2} \exp\left(\frac{-m({v_x}^2+{v_y}^2+{v_z}^2)}{2kT^\circ}\right). \qquad \text{(A7)}$$

Using the definition of *v* above, this joint distribution in Cartesian coordinates is:

$$f(v_x v_y v_z)dv = \left(\frac{m}{2\pi kT^\circ}\right)^{\frac{3}{2}} \exp\left(\frac{-mv^2}{2kT^\circ}\right) dv_x dv_y dv_z.$$

The three directions of the differential as *dv* in spherical coordinates are *v*, $vd\theta$, $vsin(\theta)d\phi$, respectively. These replace the differentials $dv_x dv_y dv_z$ so that:

$$dv_x dv_y dv_z = dv(vd\theta)(v\sin(\theta)d\phi).$$

$$f(v_x v_y v_z)dv = \left(\frac{m}{2\pi kT^\circ}\right)^{\frac{3}{2}} \exp\left(\frac{-mv^2}{2kT^\circ}\right) dv_x dv_y dv_z$$

$$f\big((v_x v_y v_z)\big)dv = \left(\frac{m}{2\pi kT^\circ}\right)^{3/2} \exp\left(\frac{-mv^2}{2kT^\circ}\right) v^2 dv(d\theta)\sin(\theta)d\phi. \qquad \text{(A8)}$$

Integrating the joint distribution in (A8) over the two angles produces the marginal velocity distribution, *f*(*v*):

$$f(v) = \left(\frac{m}{2\pi kT^\circ}\right)^{\frac{3}{2}} \exp\left(\frac{-mv^2}{2kT^\circ}\right) v^2 \int_0^\pi \int_0^{2\pi} v^2 \, d\theta \sin(\theta) d\phi dv \qquad \text{(A9)}$$

The double integral is the spherical shell volume of $(4\pi)v^2$. This marginal velocity distribution becomes the familiar Maxwell-Boltzmann distribution listed in the text as (2):

$$f(v) = \left(\frac{m}{2\pi kT^\circ}\right)^{\frac{3}{2}} (4\pi)v^2 \exp\left(\frac{-mv^2}{2kT^\circ}\right) \qquad (2)$$

Most of the equations and concepts in the above development can be found from references [10], [18], and the instructional website, Hyperphysics:
http://hyperphysics.phy-astr.gsu.edu/hbase/quantum/disfcn.html#c2
http://hyperphysics.phy-astr.gsu.edu/hbase/Kinetic/kintem.html#c5.

Appendix B

Development of the Energy Distribution from the MB Velocity Distribution

The relationship between energy and velocity in (5) is used to find the distribution for E from the MB pdf in (2) applying the change of variable technique (from v to E):

$$E = \left(\frac{1}{2}\right) m v^2 \tag{5}$$

where m is reduced mass expressed as: $m_1 m_2/(m_1+m_2)$. This kinetic energy definition with this mass definition is often referred to as the center-of-energy, or E_{CM}.

The Jacobian of that transformation is

$$J = \frac{dv}{dE} = \sqrt{\frac{1}{2mE}} \ , \tag{B1}$$

The pdf for E is found by substituting

$$v = \sqrt{\frac{2E}{m}} \tag{B2}$$

into (5), the MB velocity pdf,

$$g(v)dv = 4\pi \left(\frac{m}{2\pi k T^\circ}\right)^{1.5} v^2 \exp\left(\frac{-mv^2}{2kT^\circ}\right) dv \quad , \tag{B3}$$

and multiplying the result by the Jacobian in (B2):

$$g(E) = g(v) \cdot J$$

$$g(E) = \left(\frac{2}{\pi}\right)^{1/2} \left(\frac{m}{T}\right)^{3/2} \frac{2E}{m} exp\left(-\frac{m2E}{m2T}\right) \sqrt{\frac{1}{2mE}} \quad . \tag{B4}$$

Simplifying (B4) produces the MB-based energy distribution as shown in the text in (7):

$$g(E) = 2\left(\frac{E}{\pi}\right)^{1/2} \left(\frac{1}{T}\right)^{3/2} exp\left(-\frac{E}{T}\right). \tag{B5}$$

Wikipedia® [10] provides the development of (B5) from the momentum, p, in (6):

$$E = \left(\frac{|p|^2}{2m}\right). \tag{6}$$

Appendix C
Development of Alternative Constant Cross-Section Case

The constant cross-section special case began with defining $h(E)$ as (25):

$$h(E) = \left(\frac{1}{T}\right)\exp(-E/. \tag{25}$$

This resulted in an analytical solution for the first moment because <E^*> in (26) was the mean of the exponential pdf, and that mean is T:

$$< E^* >= \int_0^\infty \frac{1}{T} E\exp(-E/T)\, dE = \tag{C1}$$

Another analytical solution was given by Gerry Hale [personal communication] using the following for $h(E)$:

$$h(E) = \exp(-E/T). \tag{C2}$$

The resulting first moment of E expression for the function in (C2) is

$$< E_2^* >= \int_0^\infty Eexp(-E/T)dE = exp(-E/T)(\frac{-E/T-1}{(\frac{1}{T})^2}). \tag{C3}$$

As (C3) indicates, this integral has an analytical solution. Its evaluation from the limits is:

$$< E_2^* >= 0\text{-}(\text{-}T^2) = T^2. \tag{C4}$$

Note that from (C3) and (C4):

$$< E_2^* >= T < E^* >. \tag{C5}$$

Dropping both the constant cross-section and leading C, the reactivity for this E_2^* is:

$$f^* = T^{-3/2} \int_0^\infty E \exp(-E/T)dE = T^{-3/2} < E_2^* >. \tag{C6}$$

The first reactivity derivative of $< E^* >$ with T in (33) is:

$$f^{*\prime} = -\frac{1}{2}\left(\frac{1}{T}\right)^{3/2} < E^* > + \left(\frac{1}{T}\right)^{5/2} < E^* >^2. \tag{33}$$

Using (C5) in (33) produces the reactivity derivative with T for E_2^*

$$f^{*\prime} = -\frac{1}{2}\left(\frac{1}{T}\right)^{3/2} \frac{< E_2^* >}{T} + \left(\frac{1}{T}\right)^{5/2} \frac{< E_2^* >^2}{T^2}$$

$$f^{*\prime} = -\frac{1}{2}T^{-5/2} < E_2^* > +T^{-9/2} < E_2^* >^2. \quad \text{(C6)}$$

Forming the f'/f ratio combines (33) with (C6) to produce the following:

$$\frac{f^{*\prime}}{f^*} = \frac{-\frac{1}{2}T^{-5/2}<E_2^*>+T^{-9/2}<E_2^*>^2}{T^{-3/2}<E_2^*>} = \frac{-1}{2T} + \frac{<E_2>}{T^3}. \quad \text{(C7)}$$

This ratio corresponds to the f'/f ratio for $<E^*>$ in (34):

$$\frac{f^{*\prime}}{f^*} = \frac{\left(-\frac{1}{2}T^{-3/2}<E^*>+T^{-5/2}<E^*>^2\right)}{T^{-1/2}<E^*>} = \frac{-1}{2T} + \frac{<E^*>}{T^2}.$$